

Curvature Ductility Factor of Reinforced Concrete Beams with Confinement under Different Strain Rates of Loading

Omar K. Alghazawi

Department of civil Engineering, Al-Ahliyya Amman University, Jordan

Received August 13, 2022; Revised November 14, 2022; Accepted December 22, 2022

Cite This Paper in the Following Citation Styles

(a): [1] Omar K. Alghazawi , "Curvature Ductility Factor of Reinforced Concrete Beams with Confinement under Different Strain Rates of Loading," *Civil Engineering and Architecture*, Vol. 11, No. 2, pp. 847 - 862, 2023. DOI: 10.13189/cea.2023.110223.

(b): Omar K. Alghazawi (2023). *Curvature Ductility Factor of Reinforced Concrete Beams with Confinement under Different Strain Rates of Loading*. *Civil Engineering and Architecture*, 11(2), 847 - 862. DOI: 10.13189/cea.2023.110223.

Copyright©2023 by authors, all rights reserved. Authors agree that this article remains permanently open access under the terms of the Creative Commons Attribution License 4.0 International License

Abstract The purpose of this work is to investigate the influence of confinement on the curvature ductility factor of reinforced concrete beams at low and high strain rates of loading. The curvature ductility of beams is affected by the tension reinforcement ratio, the compression-reinforced ratio, the compression strength of concrete f'_c , and the yield strength of steel f_y . The degree of transverse reinforcement is another component that determines beam flexural behavior. A model of steel and restricted concrete under varying strain rates of loading was utilized to compute the curvature ductility factor. The reinforced concrete section is studied in this research to determine the confinement of the beam and the different strain rates of loading. The ratio of the volume of rectangular steel hoops to the volume of the concrete core, ρ_s , represents the confinement. Six values of ρ_s are investigated to ensure an acceptable degree of ductility capacity. It is concluded that the ACI-Code balanced reinforcement ratio is impacted by confinement, and that it is lower than the ratio achieved when confinement is present. In this work, specific values of the curvature ductility factor for beam sections constructed with the ACI code were reported for $f_y = 60$ ksi (414 MPa), $f'_c = 4$ ksi (27.6 MPa). Furthermore, the maximum quantity of tension reinforcement \max influences the curvature ductility factor.

Keywords Beams, Confinement, Curvature Ductility, Ratio of Transverse Reinforcement, Strain Rate, Steel,

Balanced Reinforcement Ratio

1. Introduction

The structural reinforced concrete frame subjected to a specified motion is constructed in such a manner that the plastic hinge mechanism can form in the beams prior to the collapse of columns during strong motion. An aim for building designers is to improve the plateau in the moment-curvature plot related to inelastic response required to provide appropriate absorption capacity of dynamic energy in beams [1]. This is accomplished when the sections of the structural components have a suitable ductility capability.

Ductility in seismic design refers to the capacity of a structure or structural parts to withstand large-amplitude cyclic deformations in the inelastic region without significantly reducing strength [2]. It is represented in reinforced concrete beam sections by the available curvature ductility factor. It is defined as the quotient of ϕ_u/ϕ_y , where ϕ_y represents the curvature at first yield and ϕ_u represents the ultimate curvature determined for unconfined or confined concrete when the compression strain reaches a given limiting value.

The curvature ductility of beams is affected by the tension reinforcement ratio, the compression-reinforced

ratio, the compression strength of concrete f'_c , and the yield strength of steel f_y . The degree of transverse reinforcement is another component that determines beam flexural behavior. Several studies have shown its efficacy in columns [3,4]. Transverse reinforcement in reinforced concrete components serves three purposes: it prevents longitudinal bar lateral buckling; it acts as shear reinforcement, and it confines the compressed concrete. Concrete confinement results in a significant increase in the strength and ductility of compressed concrete, according to tests [3,4]. Stress and strain models for constrained concrete under static or dynamic loads can be created.

Park and Ruitong [6] determined the curvature ductility factor, μ_ϕ , under static loads for certain reinforced concrete sections of ACI Code beams while neglecting the influence of transverse steel reinforcement. They show that the curvature ductility factor is at least 2 for sections with the maximum longitudinal reinforcement ratio ρ_{max} , which is regulated in the ACI Code by 0.5 to 0.75 of the balanced steel ρ_b . El Haddad [7] has added to this research by including the influence of low and high strain rates of loading on the characteristics of reinforcing steel. He applied steel constitutive models produced by Shourshian et al [12] but overlooked their influence on concrete stress. He observed that the curvature ductility factor for sections with the maximum reinforcement ratio ρ_{max} recommended by the ACI Code is between 2.7 and 4.

The interpretation of the original expression of ρ_b shows the direct effect of the limiting values for compression concrete and steel stresses [1]. Ziara et al [5] shown that confinement increases the ρ_b permitted by the ACI, and they derived a relationship between the improved value of longitudinal reinforcement ratio at balanced failure state ρ'_b and ρ_b of ACI. As a result, in most cases, the longitudinal reinforcement ratio surpasses the ρ_{max} value permitted by the ACI Code.

First, the possible curvature ductility for a specific reinforced concrete beams section is computed considering the impact of confinement by transverse steel at both low and high strain rates of loading in this article. The curvature ductility factor for an ACI-designed section is calculated. Second, in the presence of confinement, a

review of the limiting balanced reinforcement ratio b is conducted, when it is proved that the maximum authorized by the ACI Code shall be implicitly impacted.

The obtained findings demonstrated true values of the curvature ductility factor for a specific beams section constructed using the ACI Code, which exceeded the values found by Park et al [6] and El Haddad [7]. On the other hand, a review of the benefits of employing transverse steel in the manufacturing of reinforced concrete beams, as well as the ductility capacity as the ratio of longitudinal bars ρ is conducted.

Most research articles investigating curvature ductility of reinforced concrete beam focused on using, concrete beams stiffened with steel plates, some carried comparison of the effect of maximum rates of tension steel, adopted by the codes, ACI, EC8 and RPA on the value of the ductility, moment-curvature behavior and the curvature ductility factor of the beam [8-11].

2. Materials and Methods

Two models are presented, namely concrete and steel models. The present study will take into account the cross sectional shape and reinforcement arrangements. Also many variables that influence the curvature ductility of reinforced beams will be investigated in this work.

2.1. Concrete Model

The concrete behavior is determined by the straining rate, the strain gradient, and the confinement [14,15]. The confinement caused by the presence of transverse reinforcement greatly improves the strength and strain of concrete [16,17]. It is affected by the following factors:

- 1) Hoops spacing, S_h ;
- 2) Longitudinal reinforcement ratio; ρ_s .
- 3) The transverse reinforcement size and kind.

Figure 1 depicts the model used for this investigation, which considers the impacts of strain rate and confinement but not the influence of the strain gradient [3].

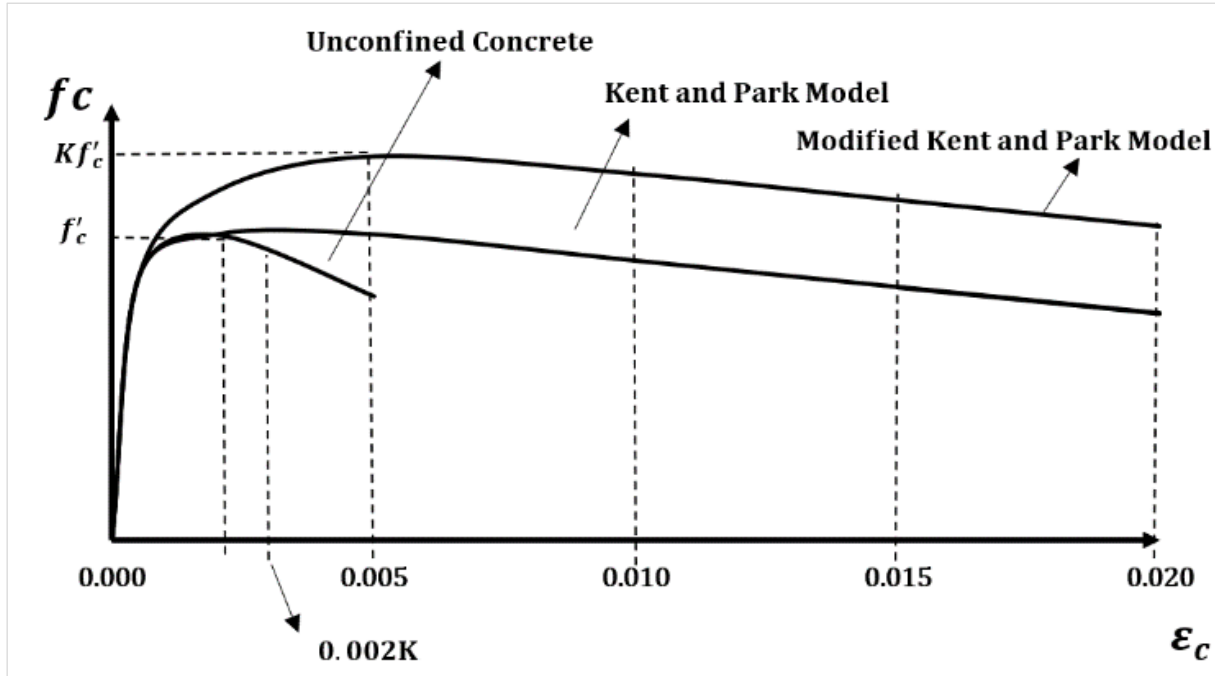


Figure 1. Assumed stress-strain relation for confined concrete [3]

The stress strain curve can be defined as follows:

For static loading and low strain rates of loading ($\dot{\epsilon} > 0.00167(1/sec)$), one can write

For $\epsilon_c \leq 0.002K$

$$f_c = Kf'_c \left[\frac{2\epsilon_c}{0.002K} - \left(\frac{\epsilon_c}{0.002K} \right)^2 \right] \quad (1)$$

$$f_c = Kf'_c [1 - Z_m (\epsilon_c - 0.002K)] \quad (2)$$

Where

$$K = 1 + \frac{\rho_s f_y h}{f'_c} \quad (3)$$

and

$$Z_m = \frac{0.5}{\frac{3+0.29 f'_c}{145 f'_c - 1000} + \frac{3}{4} \rho_s \sqrt{\frac{h''}{s_h}} - 0.002K} \quad (4)$$

On the other hand, for high strain rates of loading when $\dot{\epsilon} > 0.00167(1/sec)$, expressions (1) and (2) are still valid but K and Z_m , are to be replaced by (4):

$$K = 1.25 \left(1 + \frac{\rho_s f_y h}{f'_c} \right) \quad (5)$$

And

$$Z_m = \frac{0.625}{\frac{3+0.29 f'_c}{145 f'_c - 1000} + \frac{3}{4} \rho_s \sqrt{\frac{h''}{s_h}} - 0.002K} \quad (6)$$

In the expressions (1), (2), (3) and (4), the following definitions have been used:

ϵ_c = longitudinal strain in concrete

f'_c = concrete compressive cylinder strength (MPa, 1MPa = 145 psi)

ρ_s = ratio of transverse reinforcement ($\rho_s = A_t / S_h h''$)

f_y = yield strength of steel hoops (MPa)

h'' = width of the concrete core measured outside of the peripheral hoop (mm)

S_h = spacing of hoop sets (mm)

A_t = area of transverse reinforcement (mm²)

Several investigations [14-17] have indicated that confinement enhances the strength of the concrete core substantially, and that the peak stress of concrete under high strain rate loading rises by roughly 25% compared to the stress under low strain rate or static loading [4].

2.2. Steel Model

In the case of static loading, the steel stress-strain curve may be characterized by five parameters: the yield strength f_y , the ultimate strength f_u , the yield strain ϵ_{ys} , the strain at the beginning of the strain hardening ϵ_{SH} , and the ultimate strain ϵ_{su} as shown in Figure 2.

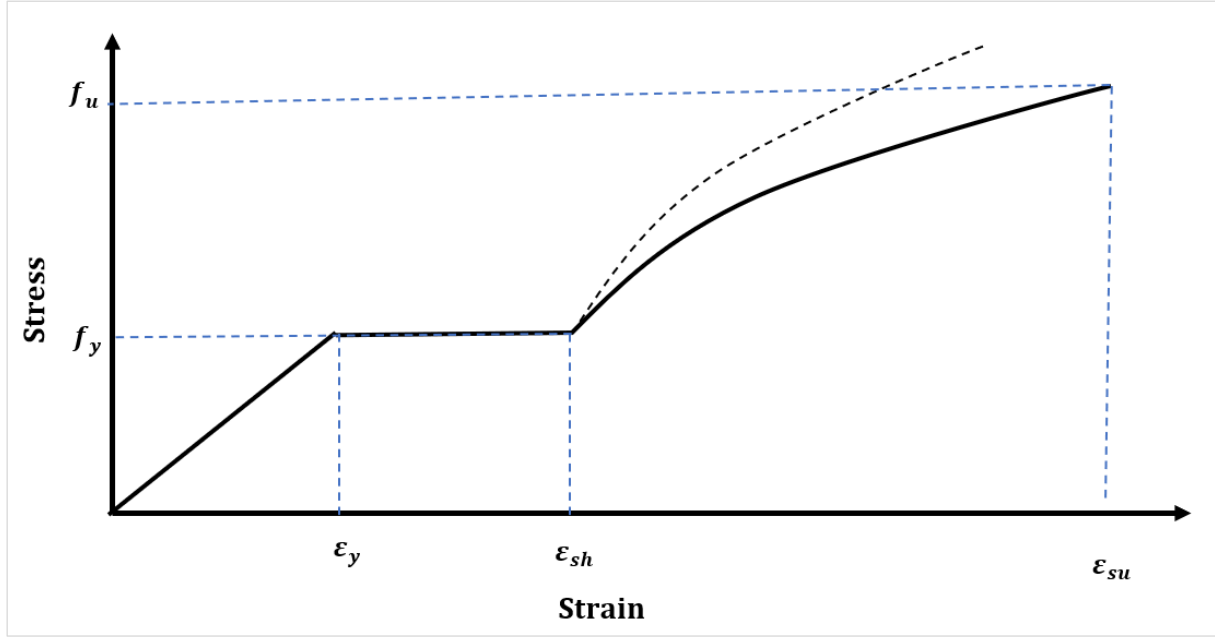


Figure 2. Typical stress-strain curves for steel reinforcement [18]

When the steel is subjected to both low and high strain rates of loading, the steel yield stress and ultimate strength rise, and the strain corresponding to these stresses either increase or remain constant as the strain rate of loading increases (8, 9). The pace of straining, however, has no effect on the steel modulus of elasticity. For the three strain ranges, the steel model behavior may be represented as follows (12, 13):

$$f_s = \begin{cases} E_s \varepsilon_s & \text{for } \varepsilon_s < \frac{f'_y}{E_s} \\ f'_y & \text{for } \frac{f'_y}{E_s} < \varepsilon_s < \varepsilon_{SH} \\ f'_y \left[\frac{112(\varepsilon_s - \varepsilon_{SH}) + 2}{60(\varepsilon_s - \varepsilon_{SH}) + 2} + \frac{(\varepsilon_s - \varepsilon_{SH})}{(\varepsilon_{su} - \varepsilon_{SH})} \left(\frac{f_u}{f'_y} - 17 \right) \right] & \text{for } \varepsilon_{SH} < \varepsilon_s < \varepsilon_{su} \end{cases} \quad (8)$$

With the expressions

$$f'_y = 3.1 + 1.2 f_y + (0.65 + 0.5 f_y) \log \dot{\varepsilon} \quad (9)$$

$$f_u = -20 + 2.5 f_y + (-2.4 + 0.12 f_y) \log \dot{\varepsilon} \geq f'_y \quad (10)$$

$$\varepsilon_{SH} = 0.12 - 0.0023 f_y + (0.02 - 0.0004 f_y) \log \dot{\varepsilon} \quad (11)$$

$$\varepsilon_{su} = 0.63 - 0.01 f_y + (0.033 - 0.00073 f_y) \log \dot{\varepsilon} \geq \varepsilon_{SH} \quad (12)$$

The following definitions are used:

- f_s : steel stress (ksi, 1 ksi=6.9 MPa)
- f_y : yield strength of steel at static loading (ksi)
- f'_y : yield strength of steel under high strain rate (ksi)
- f_u : ultimate strength of steel (ksi)
- ε_{SH} : strain corresponding to the initiation of the steel strain hardening

ε_{su} : ultimate steel strength at failure

ε_s : steel strain

E_s : steel elastic modulus ($E_s=29 \times 10^6$ or 200000 MPa)

$\dot{\varepsilon}$: strain rate of loading

2.3. Section Behavior Model

A technique initially presented in [6] considers the strain diagram and the equilibrium needs of internal and external forces to determine the possible curvature ductility factor for unconfined sections. This accounts for the non-linear behavior of unconfined compressed concrete. Figure 3 depicts the stress-strain graphs of a doubly reinforced concrete segment at the first yield, ϕ_y , and final curvature phases.

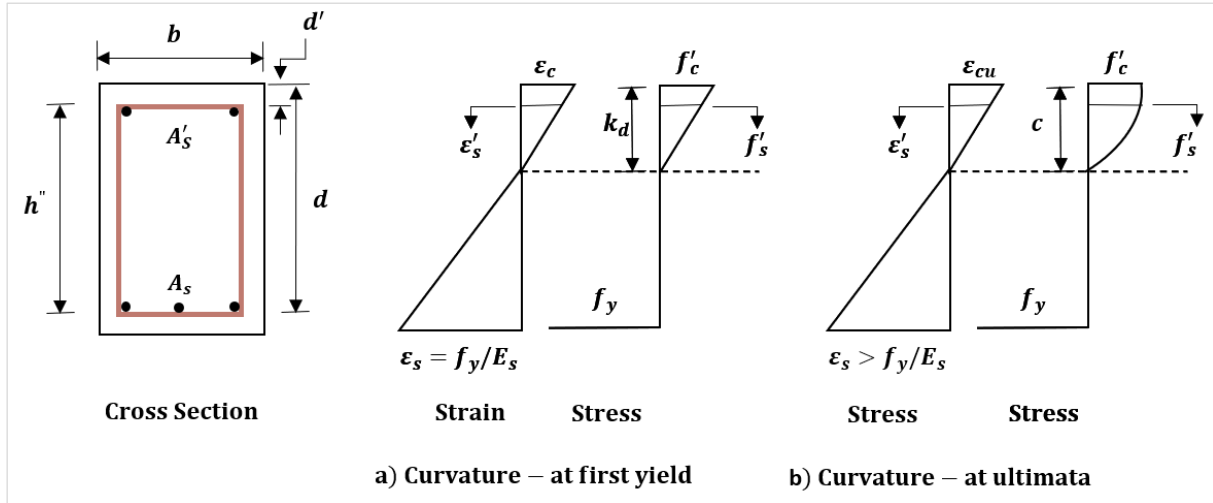


Figure 3. Reinforced concrete beam section with flexure [19]

The initial yield curvature, ϕ_y , can be stated as follows (see fig.3a):

$$\phi_y = \frac{f_y/E_s}{d(1-k)} \quad (13)$$

where k is the neutral axis depth factor at initial yield, tension steel ratio ($\rho = A_s/bd$) and compression steel ratio ($\rho' = A'_s/bd$). When concrete strain at the extreme compression fiber reaches a limiting value ϵ_{cu} , the ultimate curvature ϕ_u is determined as follows (see fig. 3b):

$$\phi_u = \frac{\epsilon_{cu}}{c} \quad (14)$$

Where c is the depth of the neutral axis. According to the ACI code [1], the limiting value of ϵ_{cu} is 0.003. Several studies have quantified the confinement impact in reinforced concrete members for increased ductility capability in the confined concrete sections [14,15,16 and 17]. Scott, Park, and Priestly [4] proposed a model for predicting the ultimate concrete compressive strain in a restricted concrete core. ϵ_{cumax} denotes the maximum available concrete compressive strain.

$$\epsilon_{cumax} = 0.004 + 0.9\rho_s \frac{f_{yh}}{300} \quad (15)$$

With f_{yh} being the hoops steel yield strength in MPa, and ρ_s is the ratio of the total volume of transverse reinforcement to the volume of concrete core. Current studies [11,12] indicate that ϵ_{cumax} always exceeds considerably the value of ϵ_{cu} for unconfined section allowed by ACI code [1], as a function of ρ_s . The factor of curvature ductility μ_ϕ for a given section will be

determined by the associated value of ϕ_u / ϕ_y .

2.4. Parametric Study of Curvature Ductility

The reinforced concrete section presented in Figure 3 will be analyzed in this study to determine the confinement of the beam and the different strain rates of loading. The ratio of the volume of rectangular steel hoops to the volume of the concrete core, ρ_s , represents the confinement. Six values of ρ_s will be investigated to ensure an acceptable degree of ductility capacity: 0.0, 0.005, 0.010, 0.015, 0.020, and 0.025. With $f_{yh}=309\text{MPa}$, the ratio of the spacing hoop S_h and the width of the concrete core measured outside of the peripheral hoop h'' is 0.5 for all these values (45ksi). This analysis will be conducted four times for four different strain rates of loading.

3. Results and Discussion

The first scenario involves static loading. The other two low strain rate loading situations are $\dot{\epsilon}=0.0000033/\text{sec}$ and $\dot{\epsilon}=0.00167/\text{sec}$. Finally, for large strain rates, we choose $\dot{\epsilon}=0.1/\text{sec}$. Figures 4–7 depict the results, which are compared in Tables 1 and 2. Each picture illustrates six curves of the computed available curvature ductility factor ρ_s versus the tension steel ratio p . The curves in figures 4a, 6a, and 7a are produced with a compression steel tension steel area ratio of 0.5. Figures 4b, 5b, 6b, and 7b show curves produced for $\rho'/\rho=0.75$.

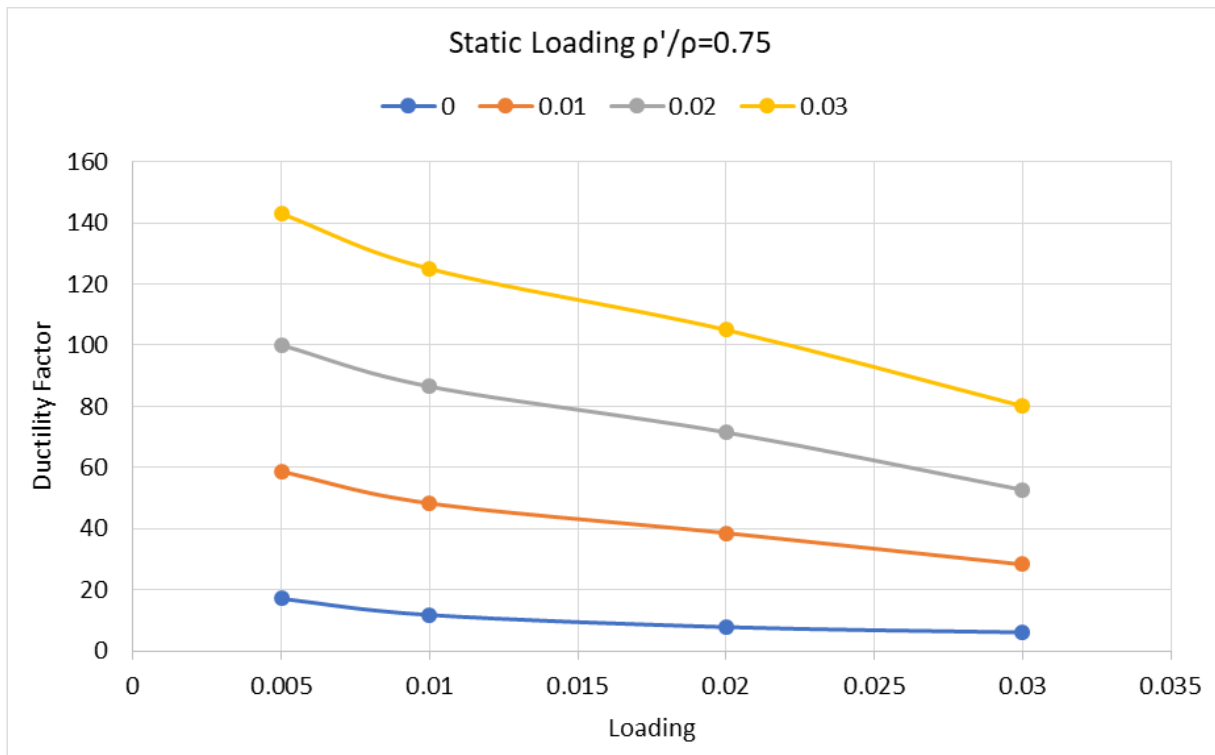
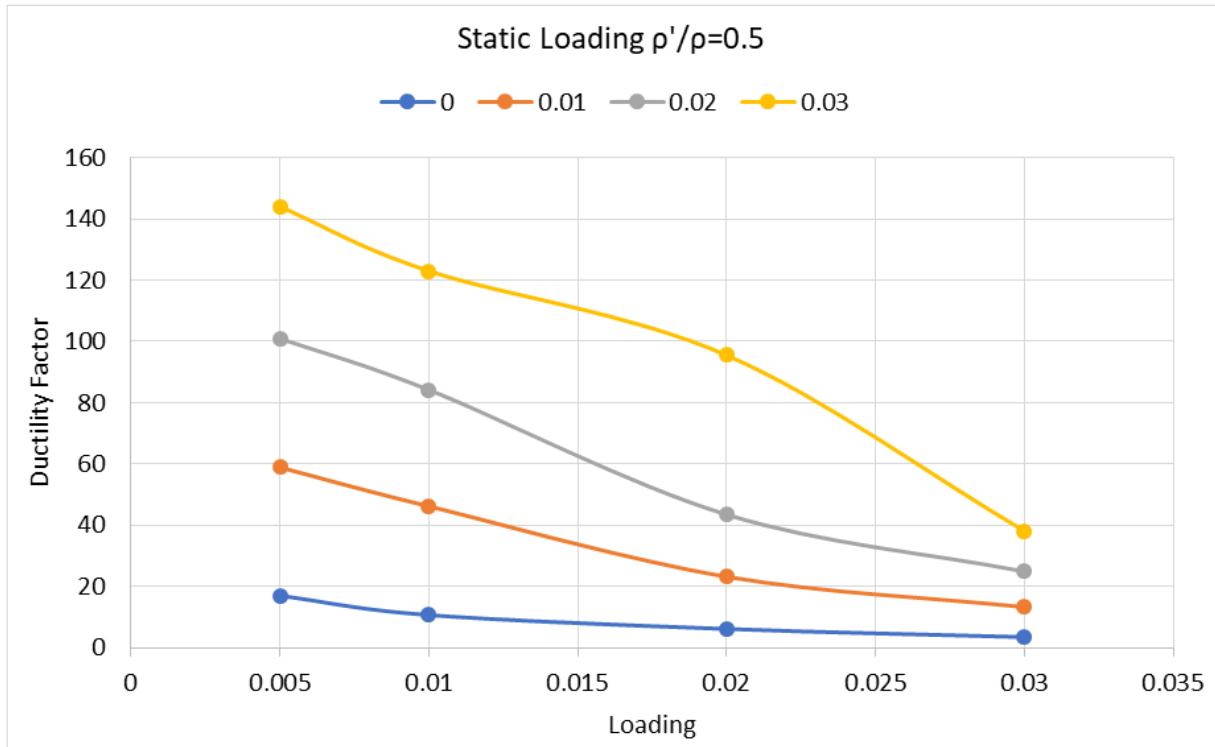


Figure 4. Part A and Part B: Variability of curvature ductility factor for reinforced concrete beams with confinement under static load

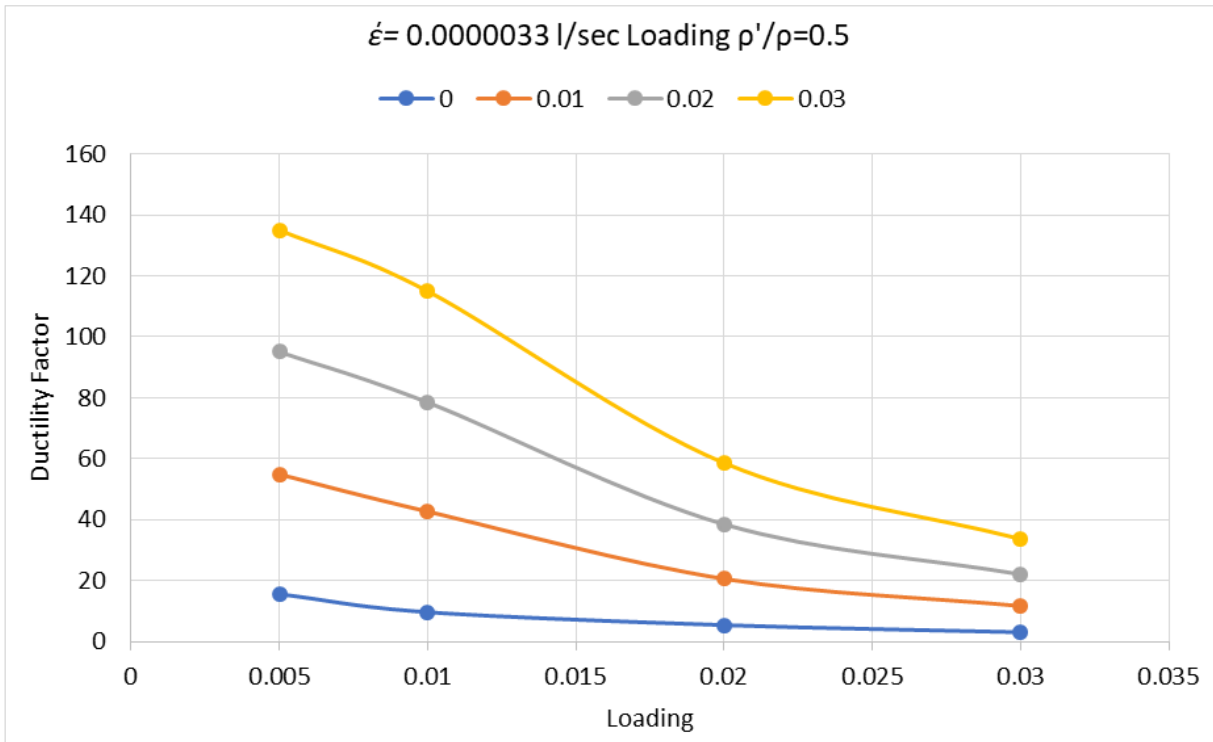
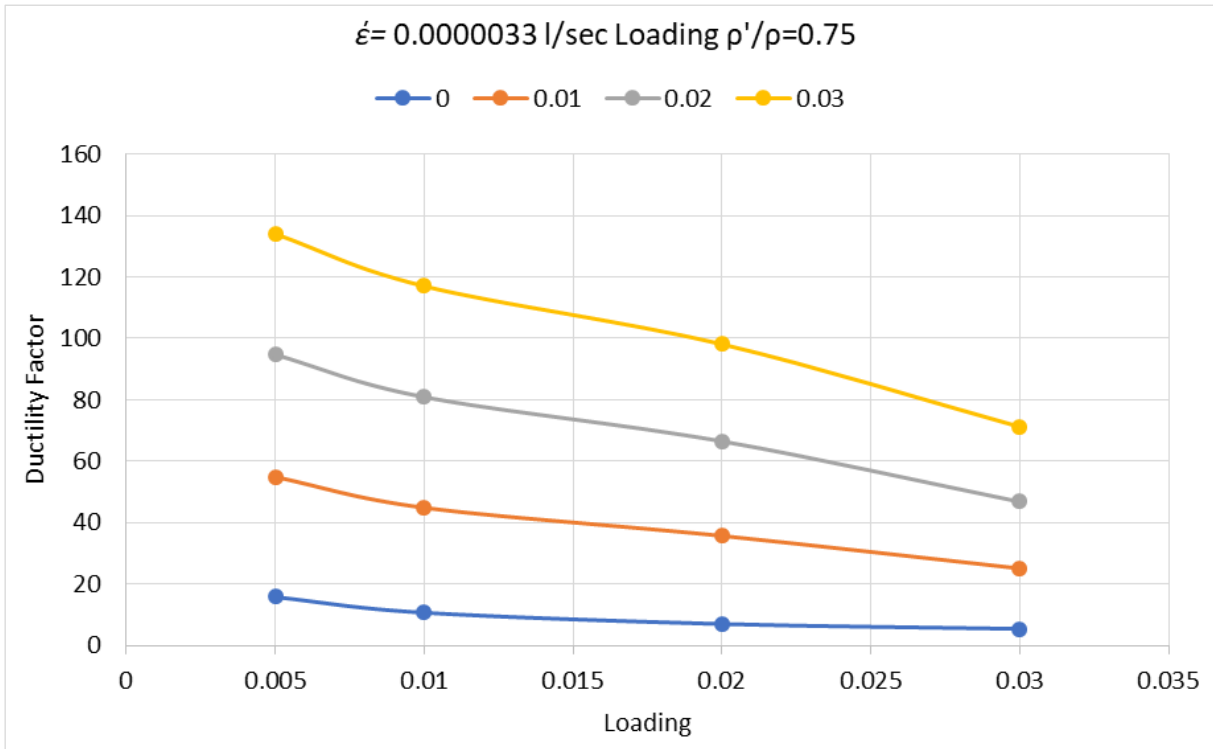


Figure 5. Part A and Part B: Variability of curvature ductility factor for reinforced concrete beams with confinement under Low strain of $\dot{\epsilon} = 0.0000033/\text{sec}$

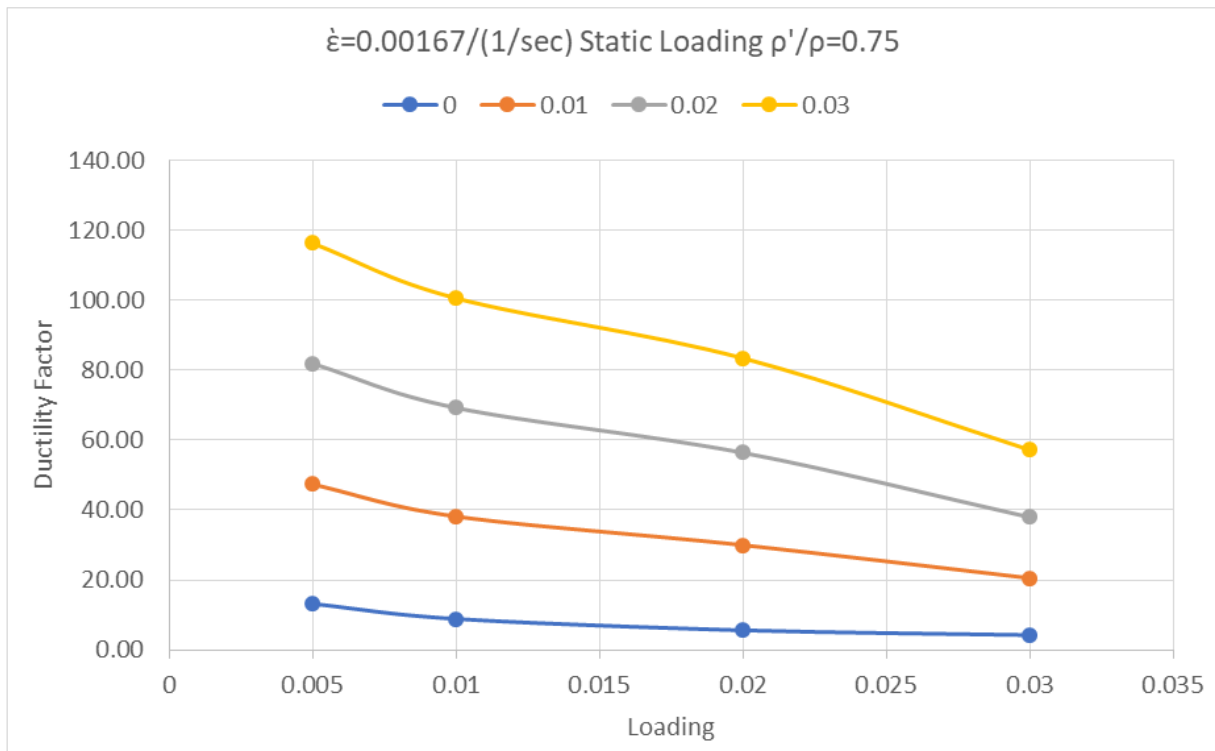
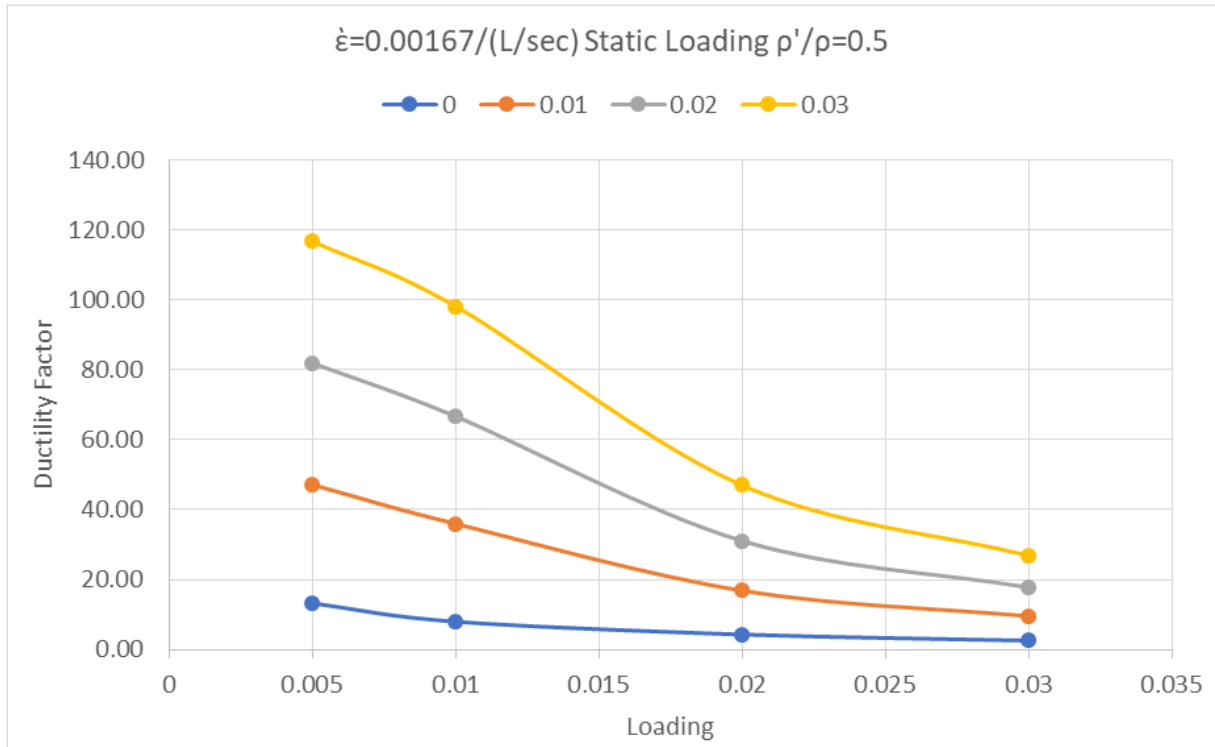


Figure 6. Part A and Part B: Variability of curvature ductility factor for reinforced concrete beams with confinement under medium strain of $\dot{\epsilon}=0.00167$ L/sec

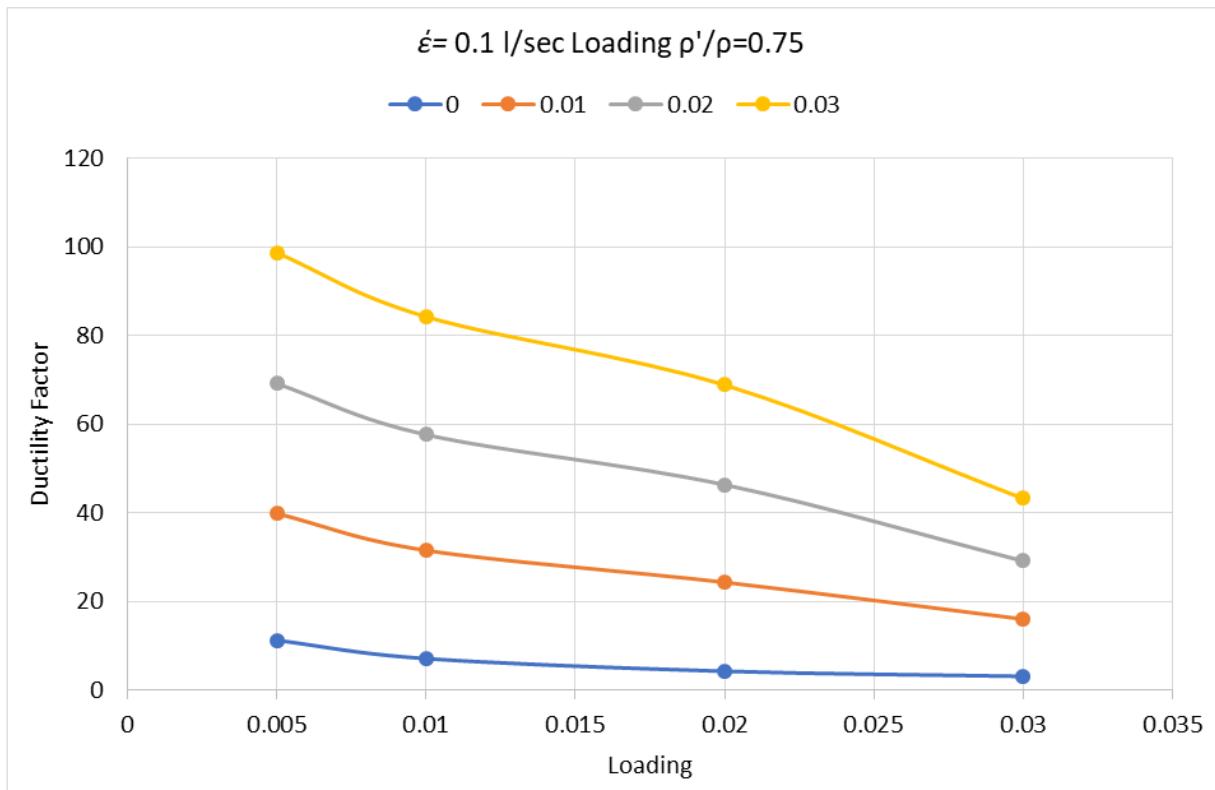
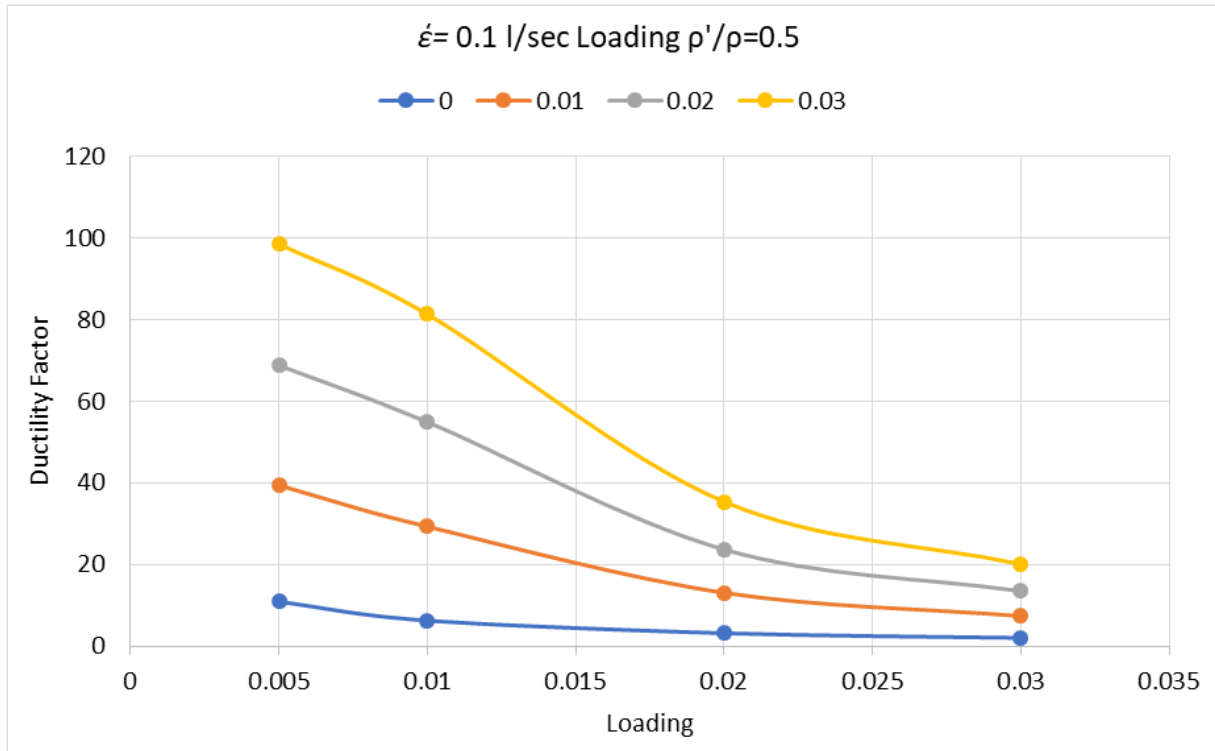


Figure 7. Part A and Part B: Variability of curvature ductility factor for reinforced concrete beams with confinement under high strain of $\dot{\epsilon} = 0.1$ /sec

Table 1. Selected results for the available curvature ductility factor μ_ϕ for beams with confinement

Loading		Static Loading				$\dot{\epsilon}=0.000033/(1/sec)$					$\dot{\epsilon}=0.00167/(1/sec)$				$\dot{\epsilon}=0.1/(1/sec)$			
ρ_s		0.00	0.01	0.02	0.03	0.00	0.01	0.02	0.03	0.00	0.01	0.02	0.03	0.00	0.01	0.02	0.03	
$\rho=$	0.005	17.00	58.90	101.20	144.00	15.60	54.90	95.10	135.00	13.25	47.15	81.95	116.75	10.90	39.40	68.80	98.50	
	0.01	10.70	46.20	84.20	123.00	9.69	42.70	78.50	115.10	8.00	36.00	66.70	98.20	6.30	29.30	54.90	81.30	
	0.02	6.15	23.20	43.50	95.50	5.44	20.60	38.50	58.60	4.32	16.85	31.10	47.00	3.19	13.10	23.70	35.40	
	0.03	3.50	13.30	24.90	38.10	3.09	11.70	22.10	33.70	2.56	9.55	17.80	26.90	2.03	7.39	13.50	20.10	

$f_y = 60$ ksi (414MPa), $f'_c = 4$ ksi (27.6 MPa), $\rho'/\rho = 0.50$

Table 2. Selected results for the available curvature ductility factor μ_ϕ for beams with confinement

Loading		Static Loading				$\dot{\epsilon}=0.000033/(1/sec)$					$\dot{\epsilon}=0.00167/(1/sec)$				$\dot{\epsilon}=0.1/(1/sec)$			
ρ_s		0.00	0.01	0.02	0.03	0.00	0.01	0.02	0.03	0.00	0.01	0.02	0.03	0.00	0.01	0.02	0.03	
$\rho=$	0.005	17.10	58.70	100.00	143.00	15.80	54.90	94.70	134.00	13.20	47.35	81.90	116.30	11.20	39.80	69.10	98.60	
	0.01	11.80	48.30	86.50	125.00	10.70	44.90	80.90	117.00	8.90	38.20	69.25	100.60	7.09	31.5	57.60	84.20	
	0.02	7.82	38.60	71.50	105.00	7.01	35.70	66.50	98.10	5.62	30.00	56.40	83.45	4.23	24.30	46.30	68.80	
	0.03	6.11	28.30	52.70	80.10	5.44	25.10	46.80	71.20	4.27	20.55	37.95	57.20	3.09	16.00	29.10	43.20	

$f_y = 60$ ksi (414MPa), $f'_c = 4$ ksi (27.6 MPa), $\rho'/\rho = 0.75$

3.1. Effect of Confinement

Figure 4a depicts the impact of confinement on a reinforced concrete section beam with various transverse reinforcement ρ_s ratios under static stress. It shows that the curvature ductility μ_ϕ increases as ρ_s increases for each curve. This is also seen by the graph, in which μ_ϕ rises when ρ decreases. Comparing portions (a) and (b) of fig. 4 reveals that compressed longitudinal steel has no influence on the curvature ductility factor μ_ϕ in the presence of confinement as the ratio ρ'/ρ grows from 0.5 to 0.75. Figures 5–7 depict these observations at various strain rates of loading.

Tables 1 and 2 validate these representations, demonstrating that μ_ϕ is about 3 to 4 times bigger than the case of limited section with $\rho_s=0.01$. In the case of static loading, this augmentation will be of order 2 when $\rho_s=0.02$. The explanation for this is because the compressive strength of the concrete increased in the presence of confinement [14,15].

3.2. Effect of Strain Rate

When the column was loaded to failure in the laboratory for 10 minutes to 2 hours, the low strain rate ($\dot{\epsilon}=0.0000033/\text{sec}$) was depicted. The strain rate of loading ($\dot{\epsilon}=0.00167/\text{sec}$) was chosen to be the midpoint between

the low and high strain rates of loading. As a result, 0.1/sec indicates the strain rate $\dot{\epsilon}$ indicated throughout the earthquake reinforced concrete reaction [4]. Figures 4–7 depict the impacts of strain rate of loading.

A quick look at figures 4a and 5a, or 6a and 7a, reveals that the curvature ductility capability μ_ϕ drops significantly as the strain rate $\dot{\epsilon}$ of loading increases. This finding is supported by a comparison of figures 4b and 5b or 6b and 7b. This pattern is visible throughout all rates of loading ranges, from static loading to high strain rates of loading. Tables 1 and 2 also indicate this variance, with a drop of roughly 30% from the static loading case to the high strain rate loading scenario. This drop is linked to an increase in the strength of reinforcing steels as strain rates of loading rise [12,13].

Figures 8–11 show the comparative variability of curvature ductility factor for reinforced concrete beams with confinement under different loading strain rates.

3.3. Influence of Confinement on the Ratio ρ_b

The quantity of tension reinforcement ρ has an influence on the ductile behavior of beams. Figures 4–7 clearly indicate that confinement has a positive influence on the curvature ductility factor. Indeed, the confinement impact on the maximum amount of tension reinforcement allowed by the ACI building code must be demonstrated [1].

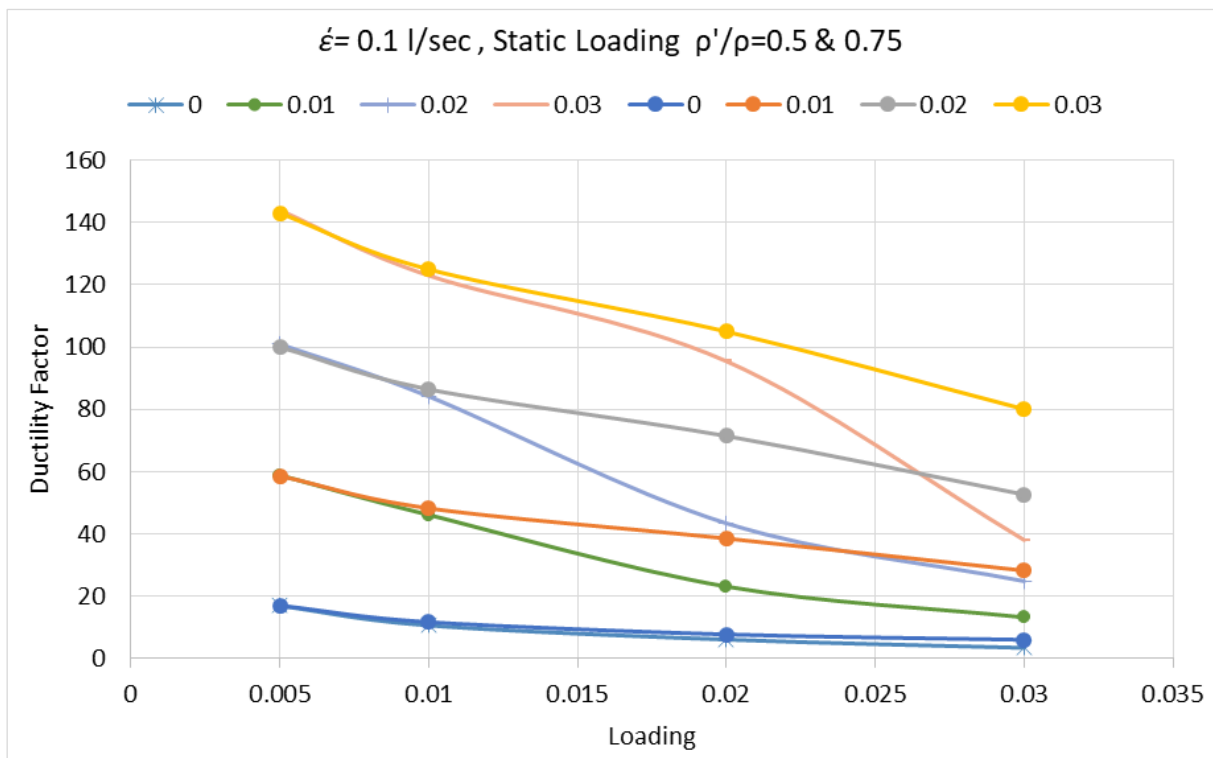


Figure 8. Comparative Variability of curvature ductility factor for reinforced concrete beams with confinement under high strain of $\dot{\epsilon}=0.1/\text{sec}$

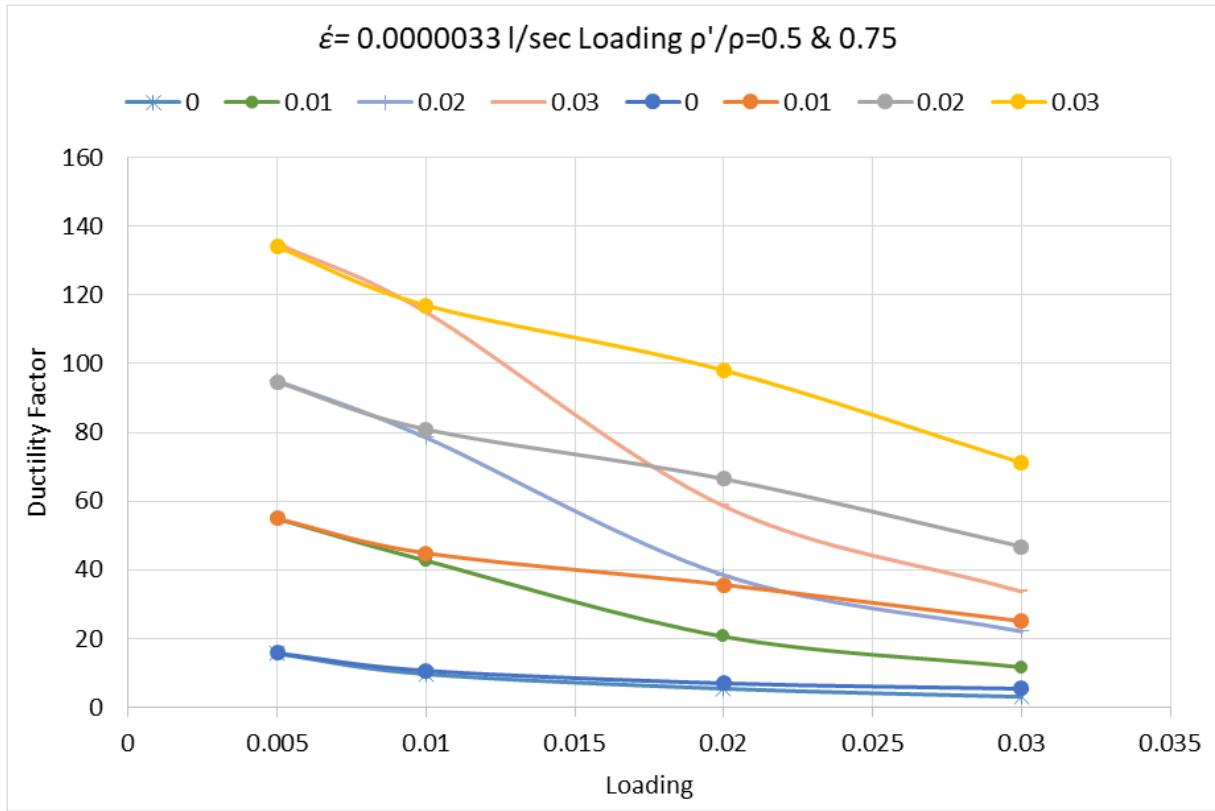


Figure 9. Comparative Variability of curvature ductility factor for reinforced concrete beams with confinement under Low strain of $\dot{\epsilon}=0.0000033/\text{sec}$

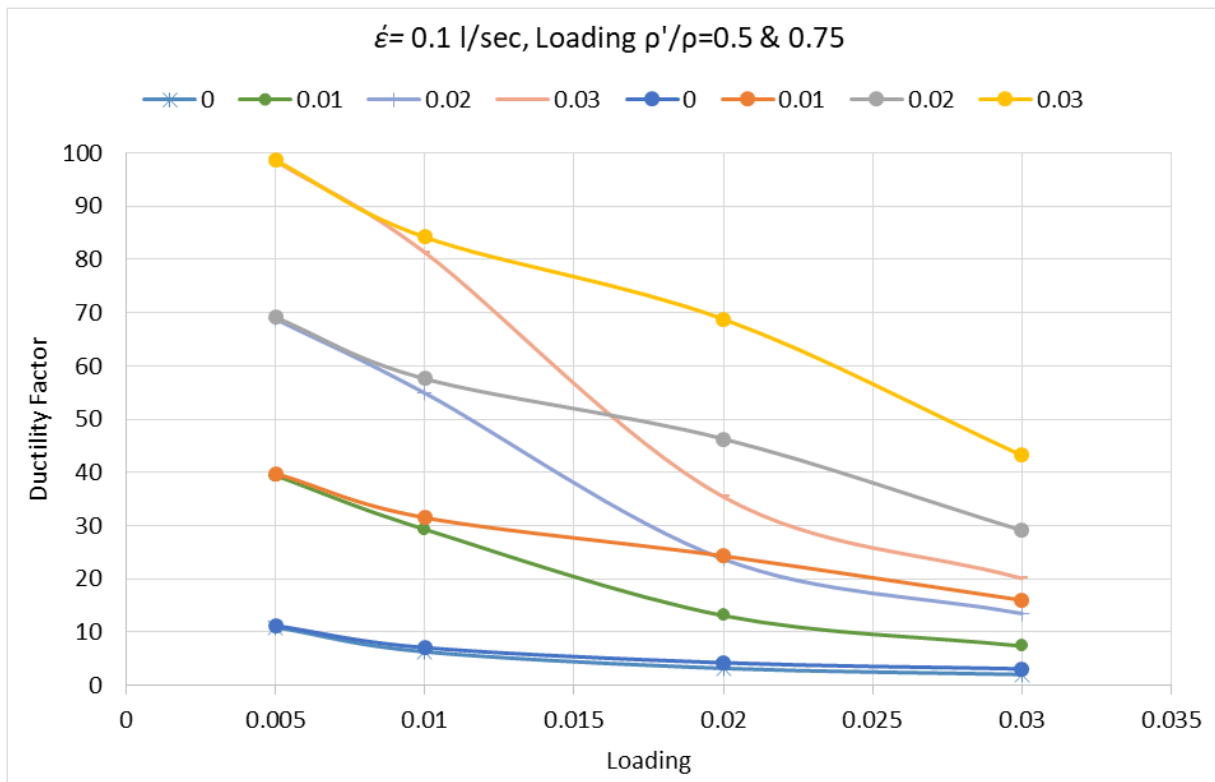


Figure 10. Comparative Variability of curvature ductility factor for reinforced concrete beams with confinement under high strain of $\dot{\epsilon}=0.1/\text{sec}$

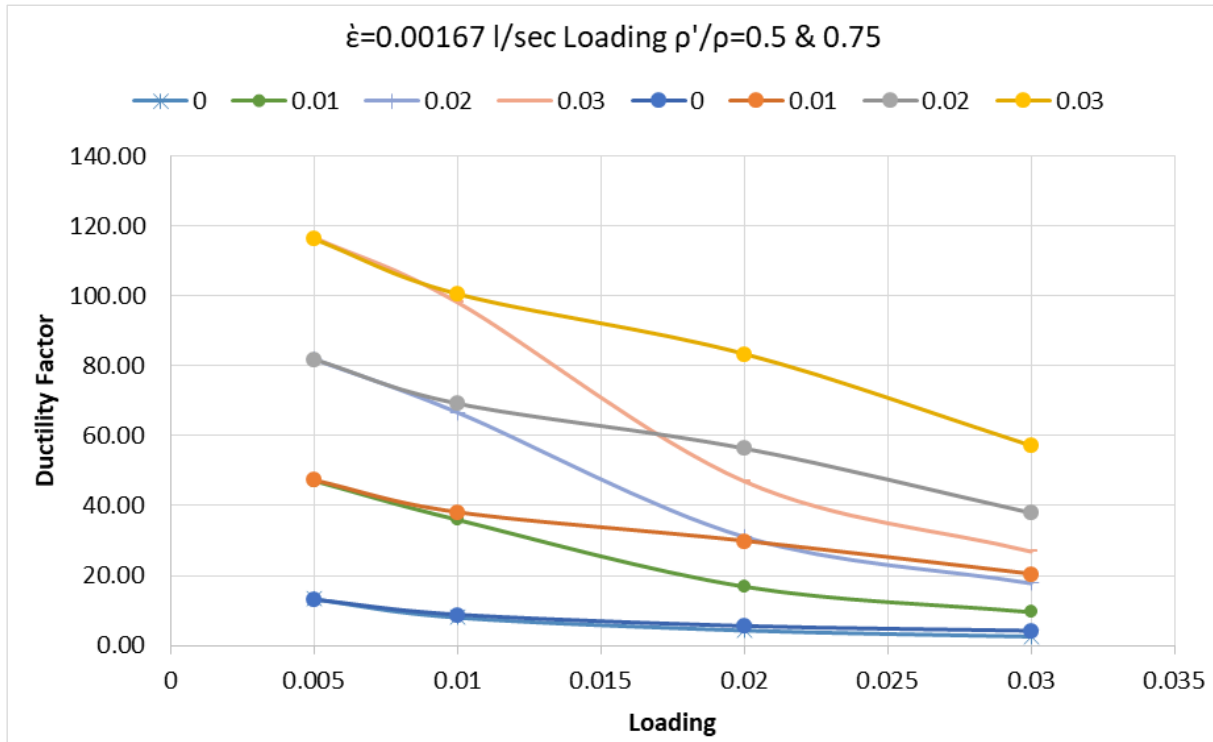


Figure 11. Comparative Variability of curvature ductility factor for reinforced concrete beams with confinement under medium strain of $\dot{\epsilon}=0.00167$ 1/sec

If the compression steel is yielding in flexural members beams sections designed with ACI code, the maximum amount of tension reinforcement ρ_{\max} is generally limited to $0.75b$, and for negative moment redistribution sections ρ_{\max} is limited to $0.5b$, where the balanced reinforcement steel ratio b is expressed by:

$$\rho_b = \frac{0.85 f'_c \beta_1}{f_y} \frac{0.003 E_s}{0.003 E_s + f_y} \quad (16)$$

The impact of transverse reinforcement is not taken into consideration in equation (16). As a result, for practical reasons, the use of transverse hoops is required in reinforced concrete beams. Ziara, Hadlane, and Kuttab [5] created a novel balanced reinforcement ratio ρ_b , comparable to ρ_b (eq 16), which accounts for the effect of confinement. This new balanced reinforced ratio for constrained core concrete may be written as follows:

$$\rho'_b = \frac{0.66 K f'_c}{f_y} \frac{0.0022 K E_s}{0.0022 K E_s + f_y} \quad (17)$$

K is the confinement enhancement factor or strength gain factor, described by the formula (3) for static loading and low strain rate loading and by the expression (5) for high strain rate loading.

Tables 3a and 3b compare ρ_b (eq 16) and ρ'_b (eq 17), for a value of $f'_c = 3$ ksi (20.7 MPa) and $f'_c = 4$ ksi (27.6 MPa) for the compressed concrete with $f_{yh} = 45$ ksi (309 MPa) for the transverse reinforcement and the five values of steel f_y . It can be shown that confinement has a minor influence on ρ_b at static loading for low values of ρ_s , while a meaningful effect can be seen for large values of ρ_s , with a variance of

roughly 15%. This variation grows as f'_c rises, where K is given by the equation (3).

Furthermore, when K is stated by the eq, the positive impact of confinement grows significantly f_{yh} under the high strain rate of loading (5). It should be noted that the influence of strain rate of loading was not considered in the values of y and f'_c .

According to this research, when beams are constructed with a high value of ρ_s and a high strain rate of loading, the quantity of maximum longitudinal reinforcement \max is not always respected.

3.4. Influence of Confinement on the Ratio ρ_b

- 1 At a value of $\rho_{\max} = 0.025$ permitted by the ACI-code [1], the curvature ductility factor μ_ϕ attains a value of 4 for the unconfined section and exceeds this value four times for the confined section with $\rho_s = 0.01$ and eight times with $\rho_s = 0.02$.
- 2 A value of μ_ϕ , equal to 5 at $\rho_{\max} = 0.75\rho_b$ permitted by ACI [1] for unconfined section μ_ϕ for the same section surpasses this value by 4 times with $\rho_s = 0.01$ and 8 times with $\rho_s = 0.02$.
- 3 At a value of $\rho_{\max} = 0.5b$ permitted by ACI, μ_ϕ attains 8 for the unconfined section and exceeds this value 4 times with $\rho_s = 0.01$ and 8 times with $\rho_s = 0.02$.
- 4 With beams reinforced by ACI-code minimum reinforcing steel ρ_{\min} , μ_ϕ is not less than 20 for unconfined concrete and surpasses this value by 5 times with the same section confined by $\rho_s = 0.02$.

Table 5 shows a comparison of calculated results achieved during static loading with chosen results obtained by Park and Riutong [6], for specific values of ρ authorized by ACI code. It has been demonstrated that with limited section, μ_ϕ significantly exceeds the value obtained by Park and Riutong [6]. However, the authors' [6] research did not consider the influence of confinement and strain rates of loading on the strength of compressed concrete.

3.5. Assessment of the Available Curvature Ductility

- 1 At a value of $\rho_{max}=0.025$ permitted by the ACI-code [1], the curvature ductility factor μ_ϕ attains a value of 4 for the unconfined section and exceeds this value four times for the confined section with $\rho_s=0.01$ and eight times with $\rho_s=0.02$.
- 2 2-A value of μ_ϕ , equal to 5 at $\rho_{max}=0.75\rho_b$ permitted by ACI [1] for unconfined section μ_ϕ for the same

- section surpasses this value by 4 times with $\rho_s = 0.01$ and 8 times with $\rho_s = 0.02$.
- 3 At a value of $\rho_{max}=0.5b$ permitted by ACI, μ_ϕ attains 8 for the unconfined section and exceeds this value 4 times with $\rho_s=0.01$ and 8 times with $\rho_s=0.02$.
- 4 With beams reinforced by ACI-code minimum reinforcing steel ρ_{min} , μ_ϕ is not less than 20 for unconfined concrete and surpasses this value by 5 times with the same section confined by $\rho_s=0.02$.

Table 5 shows a comparison of calculated results achieved during static loading with chosen results obtained by Park and Riutong [6], for specific values of ρ authorized by ACI code. It has been demonstrated that with limited section, μ_ϕ significantly exceeds the value obtained by Park and Riutong [6]. However, the authors' [6] research did not consider the influence of confinement and strain rates of loading on the strength of compressed concrete.

Table 3a. Comparison between the balanced reinforced steel ratio and enhancement ρ' , $f_y = 60$ ksi (414MPa), $f_{yh} = 45$ ksi (309 MPa), $f'_c = 3$ ksi (20.7 MPa)

f_y Ksi(MPa)	ρ_b of ACI (1)	ρ'_b from eq (17) with different values of ratio ρ_s			
		0.01	0.02	0.025	0.03
40(276)	0.0495	0.0475	0.0541	0.0574	0.0607
50(345)	0.0367	0.0348	0.0398	0.0424	0.0450
60(414)	0.0285	0.0268	0.0308	0.0328	0.0349
70(483)	0.0229	0.0214	0.0246	0.0263	0.0280

Table 3b. Comparison between the balanced reinforced steel ratio and enhancement ρ' , $f_y = 60$ ksi (414MPa), $f_{yh} = 45$ ksi (309 MPa), $f'_c = f'_c = 4$ ksi (27.6 MPa)

f_y Ksi(MPa)	ρ_b of ACI (1)	ρ'_b from eq (17) with different values of ratio ρ_s			
		0.01	0.02	0.025	0.03
40(276)	0.037	0.0372	0.0438	0.0472	0.0506
50(345)	0.028	0.0274	0.0325	0.0351	0.0377
60(414)	0.0213	0.0211	0.0252	0.0272	0.0293
70(483)	0.0172	0.0168	0.0201	0.0218	0.0236

Table 4. Curvature ductility factor for beams by the ACI Code (1) in presence of confinement and strain rates of loading, $f_y = 60$ ksi (414MPa), $f'_c = 4$ ksi (27.6 MPa), ($\rho'/\rho = 0.50$)

Loading	Static Loading			$\dot{\epsilon}=0.000033/(1/sec)$			$\dot{\epsilon}=0.1/(1/sec)$		
	0.00	0.01	0.02	0.00	0.01	0.02	0.00	0.01	0.02
ρ_s									
$\rho_{max}=0.025$	4.52	17.10	32.10	3.99	15.20	28.50	2.50	9.57	17.40
$\rho_{max}=0.75 \rho_b = 0.0214$	5.61	21.20	39.70	4.69	18.80	35.20	2.97	11.80	21.60
$\rho_{max}=0.5 \rho_b = 0.0143$	8.16	35.90	66.90	7.29	32.00	59.60	4.52	20.50	37.10

Table 5. Comparative study of selected results of curvature ductility factor at static loading, $f_y = 60$ ksi (414MPa), $f'_c = 4$ ksi (27.6 MPa)

ρ'/ρ	ρ	Park (6) with eq(13)	Our results with different values of ρ_s		
			0.00	0.01	0.02
0.5	0.116	8	9.61	43.6	80.6
	0.008	10	12.2	49.4	88.7
	0.250	4	4.52	17.1	32.2
0.75	0.015	8	9.31	42.5	77.8
	0.100	10	11.8	48.3	86.5

Table 6. Comparative study of selected results of curvature ductility factor $\dot{\epsilon}=0.1/(1/\text{sec})$, $f_y = 67$ ksi (462MPa), $f'_c = 4$ ksi (27.6 MPa), ($\rho'/\rho=0.50$)

ρ	El Haddad [7] with $\rho_s=0$	Our results with different values of ρ_s			
		0.00	0.01	0.015	0.02
0.028	2	1.8	6.8	9.6	12.4
0.016	4	3.4	14.9	20.8	27.0
0.009	6	5.9	27.2	39.1	51.2
0.007	8	7.3	30.5	43.1	55.8
0.005	10	9.6	35.4	48.8	62.4
0.004	12	11.3	38.9	52.9	67.0

3.6. Assessment of Under Dynamic Loading Conditions for $\dot{\epsilon}=0.1/\text{sec}$

The following conclusions may be drawn from Figure 7a and Table 4:

- 1- At a value of $\rho_{\max}=0.025$ permitted by ACI, μ_ϕ surpasses 2 for the unconfined section and exceeds 4 times the value for the confined section with $\rho_s=0.01$ and 8 times with $\rho_s=0.02$.
- 2- With unconfined concrete beams reinforced by $\rho_{\max}=0.75 \rho_b$, μ_ϕ achieves 3, and this number is increased four times for the identical confined section with $\rho_s=0.01$ and seven times with $\rho_s=0.02$.
- 3- For beams strengthened by $0.5\rho_b$, μ_ϕ is greater than 4. This value is obtained 5 times when $\rho_s=0.01$ and 9 times when $\rho_s=0.02$ for the restricted section.
- 4- With the unconfined section reinforced by the lowest reinforcement min authorized by ACI-code [1], μ_ϕ achieves 14 and surpasses its value for the confined section with $\rho_s=0.01$ by 3 times and by 6 times for the confined concrete section with $\rho_s=0.02$.

Table 6 compares the findings obtained at different values of s to the results obtained by El-Haddad [7] for the situation of high strain rate of loading ($\dot{\epsilon}=0.1/\text{sec}$), with $f_y=67\text{ksi}$ (462 MPa). It is seen that the values of μ_ϕ with the restricted section are significantly different from the values obtained by El-Haddad [7], even though the influence of strain rates of loading on the strength of compressed concrete is not considered in their research.

4. Conclusions

Under static loading conditions, it has been demonstrated that with limited section, μ_ϕ significantly exceeds the value obtained by other authors. Under dynamic loading conditions, it is seen that the values of μ_ϕ with the restricted section are significantly different from the values obtained by other authors.

Following the parametric investigation when beam confinement and strain rates of loading are considered, the curvature ductility factor of reinforced concrete beams constructed using the ACI-code outperforms the values derived by other authors. The balanced reinforcement steel ratio ρ_b increases significantly in the presence of confinement and loading strain rates. Also, when using confinement concrete in the design of beams, ρ_b is not always obeyed.

The following conclusions are derived from the results of this parametric study:

- When beam confinement and strain rates of loading are considered, the curvature ductility factor of reinforced concrete beams constructed using the ACI-code [1] outperforms the values derived by the authors of [6,7].
- The balanced reinforcement steel ratio ρ_b increases significantly in the presence of confinement and loading strain rates. However, when using confinement concrete in the design of beams, ρ_b is not always obeyed.

- The ACI-code requirement impacting the curvature ductility factor assures an essential plateau of ductility capability in the presence of confinement.

REFERENCES

- [1] Building Code Requirements for Structural Concrete (ACI 318-19) and Commentary. June 2019 DOI: 10.14359/51716937 Publisher: American Concrete Institute www.concrete.org, ISBN: 978-1-64195-056.
- [2] Park, R., "Evaluation of Ductility Structures and Structural Assemblages from Laboratory Testing". Bulletin of the New Zealand National Society for Earthquake Engineering, Vol. 22, No. 3, pp. 155-165, 1989.
- [3] Park, R., Priestly M. N. J., Gill, W. D., "Ductility of Square Confined Concrete Columns". Journal of the Structural Division – ASCE, Vol. 108, pp. 929-954, 1982.
- [4] Scott, B. D, Park, R., Priestly M. N. J., "Stress-Strain Behavior of Concrete Confined by Overlapping Hoops at Low and High Strain Rates". ACI-Journal, Vol. 92, pp. 13-27, 1982.
- [5] Ziara M. M., Haldane D., Kuttub A. S., Flexural behavior of beams with confinement. ACI structural journal. Jan-Feb 1995. pp. 103-114.
- [6] Park R. & Ruitong D., Ductility of doubly reinforced concrete beams sections. ACI structural journal. March-April 1988. pp. 217-225.
- [7] Al-Haddad M. S., Curvature ductility of reinforced concrete beams under low and high strain rates. ACI structural journal. Oct 1995. pp. 526-534.
- [8] Foroughi S. & Bahadir Yuksel S. "A New Approach for Determining the Curvature Ductility of Reinforced Concrete Beams", Slovak Journal of Civil Engineering Vol. 30, 2022, No. 1, 8 – 20.
- [9] Olivia M. & Mandal P. "Curvature Ductility of Reinforced Concrete Beam", Journal TEKNIK SIPIL Volume 6 No. 1, October 2015: 1 – 13.
- [10] Si Youcef Y., & Chemrouk M. "Curvature Ductility Factor of Rectangular Sections Reinforced Concrete Beams", World Academy of Science, Engineering and Technology International Journal of Civil and Environmental Engineering Vol. 6, No. 11, 2012, ISNI 0000000091950263, Pages 971-976.
- [11] Al-Azzawi T. K., Al Azzawi R. K. & Ibrahim T. H. "Curvature Ductility of Reinforced Concrete Beam Sections Stiffened With Steel Plates", Journal of Engineering Volume 13 No. 1 Pages 1153-1163, March 2007.
- [12] Soroushain, P., and Choi, K. B., "Steel Mechanical Properties at Different for Reinforced Concrete Sections". ACI-Structural Journal, Vol. 113, pp. 663-672, 1987.
- [13] Soroushain, P. And Obaseki, K., "Strain Rate-Dependent Interaction Diagrams for Reinforced Concrete Sections". ACI-Structural Journal, Vol. 83, pp. 108-116, 1986.
- [14] Kent, D.C., Park, R., "Flexural Members with Confined Concrete". Journal of the Structural Division- ASCE, Vol. 97, pp. 1969-1990, 1971.
- [15] Mander, J.B., Priestly, M.N.J., "Theoretical Stress-Strain Model for Concrete". Journal of the Structural Division-ASCE, Vol. 114, pp. 1804-1826, 1988.
- [16] Saatcioglu, M. & Razvi, S.R., Strength and ductility of confine concrete columns, ASCE Journal Structural 106: 1079-1102, 1992.
- [17] Sheikh, A. A., Uzumeri, S. M., "Analytical Model for Concrete Confinement in Tied Columns". Journal of the Structural Division – ASCE, Vol. 108, Dec-1982, pp. 2703-2722.
- [18] James M. Gere & Barry J. Goodno, "Mechanics of Materials" Book, SI Edition. Stress-Strain originated by Jacob Bernoulls (1654-1705) and J. V. Poncelet (1788-1867), 2009, Ref 1-4 pp 913.
- [19] Falah M. Wegain, "Concrete Structure Analysis and Design" Book Second Edition, Emphasizing American Concrete Institute (ACI 318-02) Inch-Pounds and SI Units, 2009